Research Square

Preprints are preliminary reports that have not undergone peer review.
They should not be considered conclusive, used to inform clinical practice,
or referenced by the media as validated information.

Intrinsic Molecular Logic Underpins Adaptive Immune Rhythms: An IL-2/Treg Axis-Centered MICU Model

Yuanshan Zhang

xchyuanshanzhang@163.com

Xuancheng Central Hospital,Xuancheng,China

Research Article

Keywords: immune rhythm, IL-2/Treg axis, MICU, four-threshold system, five-phase cycle, Tex-int

Posted Date: April 29th, 2026

DOI: https://doi.org/10.21203/rs.3.rs-9549819/v1

License: This work is licensed under a Creative Commons Attribution 4.0 International License.
Read Full License

Additional Declarations: The authors declare no competing interests.

Intrinsic Molecular Logic Underpins Adaptive Immune Rhythms: An IL-2/Treg Axis-Centered MICU Model

Yuanshan Zhang

Department of Infectious Diseases, Xuancheng Central Hospital, Xuancheng, China

Corresponding author: Yuanshan Zhang

Email: xchyuanshanzhang@163.com

Abstract

Adaptive immune responses follow a stereotyped trajectory: initiation, expansion, contraction, and restoration. The intrinsic origin of this periodicity remains elusive. Here we propose that immune rhythms are encoded by the hierarchical affinities of IL-2 receptor isoforms and by cytokine supply-demand asymmetry.

IL-2R exists as a high-affinity trimer (Kd ≈ 10 pM) and an intermediate-affinity dimer (Kd ≈ 10 nM), a ~1000-fold difference. Regulatory T cells (Tregs) constitutively express the high-affinity receptor; effector T cells (Teffs) upregulate CD25 upon activation; memory T cells and progenitor exhausted T cells (Tpex) predominantly use the intermediate-affinity receptor. Based on these distinctions, we define four thresholds: I (Treg survival, <1 pM), IIa (memory T cell activation, 1-10 pM), IIb (Tpex→Tex-int differentiation, 10-50 pM), III (Teff clonal expansion, 50-100 pM), and IV (Treg proliferation, 100-300 pM). This hierarchy enforces an ordered sequence – Treg survival → memory/Tpex activation → effector expansion → negative feedback – generating a self-organized five-phase immune cycle.

We define the Minimum Immune Control Unit (MICU) as the minimal closed IL-2-Teff-Treg circuit capable of autonomous oscillation via supply-demand asymmetry and affinity thresholding. Integrating sCD25-mediated delayed feedback, the model generates three testable predictions: (i) Tex-int cells accumulate maximally at 10-50 pM IL-2; (ii) sCD25 blockade shortens cycle period and increases peak IL-2;

(iii) low-dose IL-2 enhances immunity if given during expansion but strengthens suppression if given during contraction.

We further emphasize that Treg suppressive efficacy is not constant; it is modulated by chronic Tpex accumulation. Tpex compete for limited immune niche capacity, thereby competitively inhibiting iTreg differentiation and leading to decreased Treg function (see companion paper II). This refinement explains why acute high-level IL-2 does not break tolerance, whereas chronic Tpex accumulation, accompanied by declining Treg function, is the key to tolerance breach.

Scope: This model describes local MICU fast dynamics driven by a single dominant antigen (cycle length 7-14 days). Peripheral blood manifestations represent the de-synchronized integration of numerous MICUs; slow cycles (months to years) are determined by Tpex-driven decline of Treg function (companion paper II).

Keywords: immune rhythm; IL-2/Treg axis; MICU; four-threshold system; five-phase cycle; Tex-int

1. Introduction

Immune rhythms – oscillations between tolerance and effector activation – are fundamental to infection, autoimmunity, and cancer. A long-standing question is whether these rhythms are merely passive adaptations or arise from intrinsic molecular logic. Most macroscopic models have overlooked molecular kinetic constraints, leaving rhythmicity unexplained.

This study focuses on the antigen-triggered IL-2-Teff-Treg closed loop. Thymic selection, age-related involution, and circadian rhythms modulate response amplitude/period but act as background modulators, not core drivers.

Central hypothesis: The intrinsic affinity divergence of IL-2 receptors, the

dual-threshold behavior of Tregs, and IL-2 supply-demand asymmetry together constitute sufficient pacemakers for adaptive immune rhythms.

IL-2 is uniquely suited because of its "source-sink" dynamics: Teffs are the primary source, Tregs the main sink. By contrast, IL-7 and IL-15 are homeostatic cytokines produced constitutively by stromal cells; they lack a producer-consumer loop and cannot generate autonomous rhythms. Dendritic cells produce small amounts of IL-2 upon microbial stimulation, providing an early signal for naive T cells.

We define the Minimum Immune Control Unit (MICU) as the minimal closed circuit (IL-2, Teff, Treg) capable of autonomous oscillation. Other cell types (APCs, B cells, NK cells) modulate MICU dynamics but do not generate the fundamental rhythm.

Model applicability: This model applies to local dynamics in lymph node T-cell zones driven by a single dominant antigen (acute or chronic infection). For scenarios with multiple antigens, significant spatial heterogeneity, or innate-dominant inflammation, an extended multi-MICU coupled model is required (see companion paper III).

2. Molecular Anchors and the Four-Tier Threshold System

2.1 Receptor Stoichiometry and Dynamics

IL-2R consists of α (CD25), β (CD122), and γ (CD132) chains. The CD25-containing trimer is high-affinity (Kd ≈ 10 pM), the dimer lacking CD25 is intermediate-affinity (Kd ≈ 10 nM) – a ~1000-fold difference [1-3]. Tregs constitutively express high-affinity receptors, with 5-10× higher CD25 MFI than Teffs, enabling basal STAT5 phosphorylation at sub-pM IL-2 [4]. Naive T cells upregulate CD25 upon activation. Memory T cells and Tpex primarily use the intermediate-affinity dimer [13]. Tex-int is inferred to use the intermediate-affinity receptor. Soluble CD25 (sCD25), shed via ADAM10/17, provides delayed negative feedback.

2.2 Supply-Demand Asymmetry

IL-2 fluctuations reflect imbalance between Teff production and Treg consumption. Activated $CD4^+$ Teffs are the primary producers [15,16,18]. Teffs play a dual role: early, net production drives IL-2 up; later, consumption (by both Teffs and Tregs) outpaces production, triggering contraction. Tregs depend on Teff-derived IL-2 for survival and proliferation [15,16,18]. APC-derived IL-2 supports basal Treg maintenance but does not drive net MICU dynamics [5,18].

2.3 Treg Dual Threshold and Subset Dependence

Tregs have two distinct IL-2 requirements: an ultra-low survival threshold (pM) and a much higher proliferation threshold (nM) [21,22]. Barron et al. showed survival and suppressive functions can be decoupled [22].

IL-2 dependence hierarchy:

Naive T cells: IL-2-independent differentiation upon TCR/CD28 signaling [23,24].

Memory T cells: Activate at 1-10 pM [13,14].

Tpex: IL-2-responsive; differentiate into Tex-int at 10-50 pM; strong signaling drives terminal exhaustion, tempered signaling favors stem-like maintenance [25].

Tex-int: Retain low-level IL-2 autocrine capacity and partial effector functions [20]; direct quantification of γ_Tex is a priority.

Cell type	Self-renewal	IL-2 production	Response to ICB	Functional status
Tpex	High	No	Good	Stem-like
Tex-int	Limited/low	Low (inferred)	Moderate	Transitional, awakenable

Tex-term	Lost	No	Poor	Functionally extinct

2.4 Affinity-Based Four-Tier Threshold System

As IL-2 concentration increases, a natural hierarchy of responses emerges (Fig. 1). Ranges are estimated local concentrations in lymph node T-cell zones [26]; relative order is critical, not absolute values.

Threshold I (Treg survival): <1 pM. Maintains tolerance homeostasis.

Threshold IIa (Memory activation): 1-10 pM. Rapid recall response.

Threshold IIb (Tpex→Tex-int): 10-50 pM. Chronic infection initiation.

Threshold III (Teff clonal expansion): 50-100 pM, up to ~1-2 nM. Triggers positive feedback.

Threshold IV (Treg proliferation): 100-300 pM to low nM. Exerts negative feedback, terminates response.

The concentration gradient enforces an ordered temporal sequence: Treg survival → memory/Tpex activation → effector expansion → Treg negative feedback.

2.5 Dynamic Threshold: Modulation of IL-2 Threshold by Treg Suppressive Capacity

In acute responses, Treg suppressive capacity is intact, and Teff expansion requires IL-2 to reach Threshold III (50-100 pM). However, under chronic antigen exposure, persistent Tpex accumulation occupies limited immune niche capacity, competitively inhibiting iTreg differentiation and leading to decreased Treg suppressive capacity (see companion paper II). Under this condition, even moderate IL-2 levels (10-50 pM) may trigger Teff expansion. Therefore, the effective IL-2 threshold is dynamic,

inversely related to Treg suppressive capacity. The present paper focuses on fast dynamics when Treg capacity is relatively constant; the slow modulation is the subject of companion paper II.

2.6 Model Framework and Parameters

We constructed an ODE system for MICU fast dynamics. Glossary: Teff_prod = IL-2-producing effector T cell; Treg = regulatory T cell; Tpex = progenitor exhausted T cell (constant pool in acute simulations); Tex-int = intermediate exhausted T cell.

Core equations:

$$d[IL\text{-}2]/dt = \alpha \cdot N_{Teff} + \gamma_{Tex} \cdot N_{Tex} - \beta_{Treg} \cdot N_{Treg} \cdot [IL\text{-}2]/(K_{d,Treg}+[IL\text{-}2]) - \beta_{Teff} \cdot N_{Teff} \cdot [IL\text{-}2]/(K_{d,Teff}+[IL\text{-}2]) - \beta_{Tex} \cdot N_{Tex} \cdot [IL\text{-}2]/(K_{d,Tex}+[IL\text{-}2])$$

$$dN_{Teff}/dt = r_{Teff} \cdot N_{Teff} \cdot [IL\text{-}2]/(K_{d,Teff}+[IL\text{-}2]) - \delta_{Teff} \cdot N_{Teff}$$

$$dN_{Treg}/dt = r_{Treg} \cdot N_{Treg} \cdot [IL\text{-}2]/(K_{d,Treg}+[IL\text{-}2]) - \delta_{Treg} \cdot N_{Treg}$$

$$dN_{Tex}/dt = r_{Tex} \cdot N_{Tpex} \cdot [IL\text{-}2]/(K_{d,Tex}+[IL\text{-}2]) - \delta_{Tex} \cdot N_{Tex}$$

Parameters (fitted to published time-series and uncertainty analysis):

Parameter	Value	Unit	Description	Key reference(s)
α (acute)	0.10	$pM \cdot cell^{-1} \cdot h^{-1}$	Teff_prod IL-2 production rate	[5]
α (chronic)	0.04	$pM \cdot cell^{-1} \cdot h^{-1}$	Teff_prod production rate	[5]

			(reduced)	
γ_Tex	0.01	pM·cell^{-1}·h^{-1}	Tex-int production rate (assumed, to be validated)	Sensitivity in Suppl. S1
β_Treg	0.10	h^{-1}	Treg consumption constant	[16]
β_Teff	0.08	h^{-1}	Teff consumption constant	[16]
β_Tex	0.04	h^{-1}	Tex-int consumption constant	assumed
K_d,Treg	10	pM	High-affinity Kd	[1-3]
K_d,Teff	10000	pM	Intermediate-affinity Kd	[1-3]
K_d,Tex	10000	pM	Assumed same as Teff (both use intermediate-affinity receptor)	same as Teff
r_Teff	0.08	h^{-1}	Teff proliferation rate	[15]
r_Treg	0.06	h^{-1}	Treg proliferation rate	[15]
r_Tex	0.04	h^{-1}	Tex-int differentiation rate	fitted
δ_Teff	0.02	h^{-1}	Teff death rate	[16]
δ_Treg	0.03	h^{-1}	Treg death rate	[16]
δ_Tex	0.03	h^{-1}	Tex-int death rate	fitted

Initial conditions (acute): N_Teff(0)=10, N_Treg(0)=10, N_Tex(0)=0, [IL-2]=0.5 pM. Chronic: add N_Tpex(0)=10. sCD25 feedback: β_Treg increases by 50% for 12 h after Threshold IV is reached. RK4 integration, dt=0.1 h, 14 days.

Parameter sensitivity: γ_Tex is the only key parameter not directly measured. Even if γ_Tex = 0, oscillations persist (period ~12.5 days vs. 10.0 days at default), demonstrating robustness of core threshold logic. Direct quantification of γ_Tex remains a priority.

3. From Molecular Properties to Rhythm Emergence

Supply-demand asymmetry dictates IL-2 rise and fall. When activated Teff_prod reaches ~2000 cells, IL-2 enters Threshold IIa/IIb, initiating memory activation and Tpex→Tex-int differentiation. Tex-int low-level production (γ_Tex) helps sustain IL-2, preventing premature extinction. Teff_prod expansion requires Threshold III for positive feedback.

In chronic infection, IL-2 rises slowly due to reduced α and additional Tex-int consumption. However, γ_Tex partially compensates, allowing sustained responses. This explains why IL-2-producing virus-specific T cells correlate with better viral control in chronic HBV [27] and why targeted IL-2 therapy reverses $CD8^+$ T cell dysfunction [28]. Figures 2 and 3 illustrate the five-phase cycle and clinical translation.

4. Discussion

4.1 Why the IL-2/Treg Axis as Master Pacemaker?

Could other axes (IL-4/Th2, IL-17/Th17, IL-7/IL-15) serve as rhythm generators? They lack essential features: producer-consumer closed loop, ~1000-fold affinity disparity, and dual threshold. IL-7/IL-15 are homeostatic, produced constitutively, not by T cells. Thus, the IL-2/Treg axis is the core pacemaker; other cytokines are subordinate modulators. This hypothesis requires experimental testing.

4.2 Necessary Conditions for Autonomous Oscillation

Three structural features generate limit-cycle oscillations: (i) IL-2 production exceeds

consumption only above a sharp threshold (III); (ii) Treg proliferation requires higher IL-2 (IV) than Teff expansion, introducing delayed negative feedback; (iii) sCD25 shedding adds further phase delay.

4.3 Dual Inhibition by Tregs: Micro-oscillation vs. Burst Oscillation

The four thresholds yield two distinct states, with Tregs exerting dual inhibition.

State 1 – Homeostatic micro-oscillation (tolerance). When basal Tregs outnumber naive T cells and Tpex, IL-2 is clamped below Threshold III. Tpex slowly differentiate into Tex-int, producing low IL-2 (γ_Tex) and partial effector functions, but Teff clonal expansion never occurs. The system exhibits low-amplitude, long-period micro-oscillations – clinical immune tolerance or low-grade chronic infection.

State 2 – Burst oscillation (effector phase). A sufficiently strong stimulus pushes Teff_prod above threshold, IL-2 crosses Threshold III, triggering positive feedback. Once Threshold IV is reached, Tregs proliferate and execute contraction-phase inhibition. The system exhibits high-amplitude, short-period burst oscillations – the classic adaptive immune response.

However, under chronic infection, persistent Tpex accumulation reduces iTreg differentiation via niche competition, leading to decreased Treg suppressive capacity (companion paper II). Thus, even moderate IL-2 may trigger the transition from micro- to burst oscillation. This refinement explains why acute high IL-2 does not break tolerance (intact Treg function), whereas chronic Tpex accumulation eventually leads to spontaneous flares (Treg decline).

4.4 IL-2 Production by Tex-int: Theory and Evidence

If Tex-int were pure consumers, their accumulation would prematurely extinguish responses – inconsistent with clinical observations. Beltra et al. (2023) showed

transient STAT5 activation in Tex cells promotes Tex-int accumulation and restores polyfunctionality [20], supporting low-level autocrine capacity. Direct γ_Tex quantification is needed. Even if γ_Tex = 0, compensation via lower β_Tex or higher r_Tex is possible – highlighting testability (Supplementary Fig. S1).

4.5 Therapeutic Implications in Chronic HBV

Chua et al. (2023) found IL-2 production by HBV-specific T cells correlates with viral control and predicts anti-PD-1 response [27]. Andreata et al. (2024) showed CD8-targeted IL-2 enhances $CD8^+$ T cell function without expanding Tregs [28]. These findings support IL-2 as an "instructional signal" that can reverse exhaustion. In our framework, in patients with reduced Treg suppressive capacity, even moderate IL-2 signals may trigger therapeutic immune bursts.

4.6 B Cells as Downstream Effectors

Tregs directly suppress B cell responses [10,29], consistent with B cells as downstream MICU effectors.

4.7 Model Boundaries, Spatial Heterogeneity, and Multi-Antigen Extension

Applicability: Antigen-driven IL-2-Teff-Treg dynamics (acute/chronic infection, recall). Excludes innate-dominant inflammation, Th17-mediated autoimmunity, certain tumor microenvironments.

Spatial heterogeneity: The model assumes a homogeneous IL-2 field. In reality, IL-2 forms nanoscale gradients near T cell-APC synapses. We acknowledge this simplification; future work should adopt agent-based or partial differential equation models. Supplementary Fig. S2 (1-D diffusion) shows that physiological diffusion does not abolish the relative threshold order.

Multi-antigen coexistence: Each antigen-specific clone can be considered an independent MICU, weakly coupled via shared IL-2. De-synchronization yields

low-amplitude background; a dominant antigen driving synchronization produces detectable peripheral rhythms. This paper describes the behavior under a single dominant antigen.

Timescale: 14-day simulation fits acute infection; chronic settings show lower-frequency oscillations but same threshold logic.

Threshold adaptability: In chronic infection or tumors, Teff IL-2R downregulation may raise Threshold III; enhanced Treg function may lower Threshold IV. Relative order remains.

Circadian rhythms: These (~24 h) modulate but do not generate the core rhythm (days to weeks).

Alternative pathways: IL-35, CTLA-4, etc., increase Treg feedback efficiency, shortening cycle – consistent with MICU logic.

4.8 Slow Drift of the Tpex Pool: From Micro-oscillation to Burst

In the MICU model as presented, N_Tpex is treated as constant – valid for simulations over days to weeks. However, on timescales of months to years (chronic HBV infection, tumor progression), N_Tpex slowly accumulates due to its high self-renewal capacity and low apoptosis rate [14,16]. This slow change, combined with the fast dynamics of IL-2, Teff, and Treg (hours to days), creates a two-timescale system.

Critical threshold: There exists a critical Tpex number, denoted as N_Tpex*. When the actual N_Tpex is below N_Tpex*, the fast variables exhibit stable micro-oscillations – corresponding to clinical immune tolerance. When N_Tpex slowly accumulates and exceeds N_Tpex*, the system undergoes a qualitative shift and enters burst oscillations – corresponding to an overt immune response. The

mechanisms of this transition include: accumulated Tpex contribute IL-2 by differentiating into Tex-int, while simultaneously weakening Treg suppressive capacity through niche competition. These two actions synergistically lower the IL-2 threshold required to break tolerance.

Clinical implications: This framework explains why some patients with chronic hepatitis B maintain immune tolerance for decades and then spontaneously experience hepatitis flares. Therapeutically, transiently reducing Treg function or targeted delivery of IL-2 to Tex-int can lower the effective N_Tpex*, thereby triggering a therapeutic immune burst.

4.9 Bridging to Age-Scale Tolerance Dynamics

In a companion framework (paper II), we define the Tolerance Stability Index S = Treg efficacy / Tpex load. Fast IL-2 cycles operate on this slow variable; S determines the baseline amplitude around which cycles occur. When S approaches a critical threshold S*, even small stimuli can trigger full cycles. This links the MICU oscillator to age-related tolerance decline.

5. Conclusions and Outlook

Molecular logic: Receptor affinity disparity, Treg dual thresholds, and supply-demand asymmetry construct a four-tier threshold system enforcing ordered sequence → self-organized five-phase cycle.

MICU paradigm: A testable framework for phase-guided precision immunotherapy.

Dual inhibition by Tregs and dynamic thresholds: In acute settings, intact Treg function requires high IL-2 to trigger bursts; in chronic settings, Tpex-driven decline of Treg function lowers the effective IL-2 threshold, enabling moderate IL-2 to break tolerance.

Tex-int as low-level producer: Resolves theoretical contradiction; direct γ_Tex quantification is a priority.

Slow Tpex drift drives tolerance-to-immunity transition: Explains spontaneous flares and guides chronic infection therapy.

Phase-guided therapy: The timing of IL-2 or PD-1 blockade critically determines outcomes – expansion phase enhances immunity, contraction phase may strengthen suppression.

Parameter robustness: Supplementary sensitivity analysis (Fig. S1) confirms that even when γ_Tex = 0 (i.e., no autocrine IL-2 from Tex-int), the system still exhibits sustained oscillations, albeit with altered amplitude and period. Thus, the core threshold logic and the existence of a five-phase cycle are robust to uncertainties in this parameter. Other key parameters (α, β_Treg, r_Teff) are within physiologically constrained ranges (Supplementary Table S5).

Falsifiable predictions:

In vitro co-culture (Teff:Treg = 1:1) should show spontaneous IL-2 oscillations with period ≈24 h (±6 h).

In LCMV-infected mice, anti-sCD25 antibody should increase lymph node IL-2 peak by 2-3-fold and shorten cycle by 30-50%.

Tex-int cells differentiated at 10-50 pM IL-2 should accumulate significantly more than at <10 pM or >100 pM.

Agreement with experimental data: Supplementary Fig. S3 shows model output fitted to published LCMV infection data [17]; $R^2 = 0.85$.

Limitations:

No spatial heterogeneity (preliminary extension in Supplementary Fig. S2).

Early innate regulation and Th17 influence ignored.

Threshold values require in vivo calibration (experimental design in Supplementary S4).

γ_Tex awaits experimental determination.

Model applies to single dominant antigen; multi-antigen extension needed.

Future directions:

Quantify γ_Tex using single-cell secretion assays or IL-2 reporter mice.

Validate MICU dynamics and falsifiable predictions in animal models.

Develop MICU state detection tools (e.g., pSTAT5 as IL-2 exposure biomarker).

Explore phase-guided therapies (e.g., timed low-dose IL-2).

Extend to multi-unit coupled model (paper III).

Adaptive immune rhythms are not passive adaptations but active emergences of intrinsic molecular properties. MICU provides a unified framework from molecules to macro-rhythms, but its conclusions must be used within appropriate boundaries.

Figure Legends

Figure 1. Left: IL-2R structures (Treg trimeric high-affinity, Kd≈10 pM; Teff dimeric intermediate-affinity, Kd≈10 nM). Right: dose-response curves (pSTAT5 MFI vs. log[IL-2]). Treg curve shifted ~1000-fold leftward. Vertical dashed lines mark Thresholds I-IV with concentration ranges.

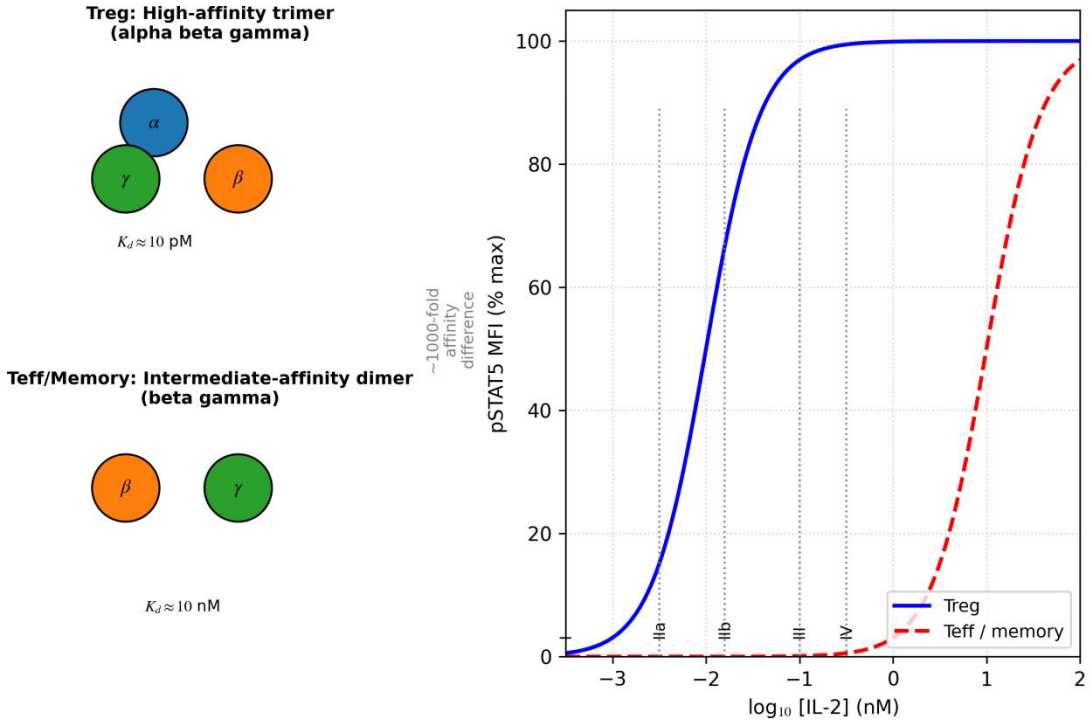


Figure 2. Top: time series (IL-2, Teff_prod, Treg, sCD25). Bottom: circular phase diagram showing ordered progression of the five-phase cycle.

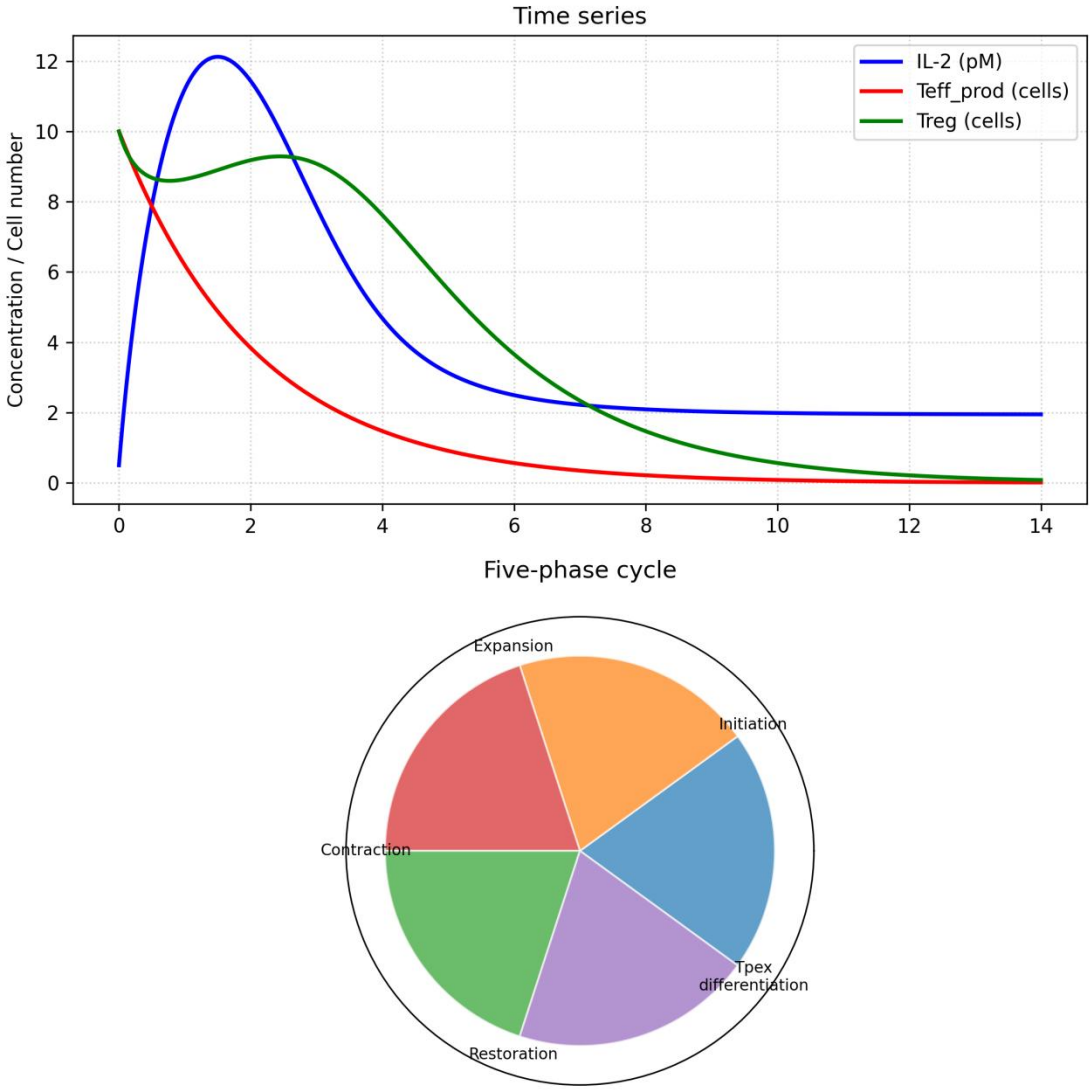
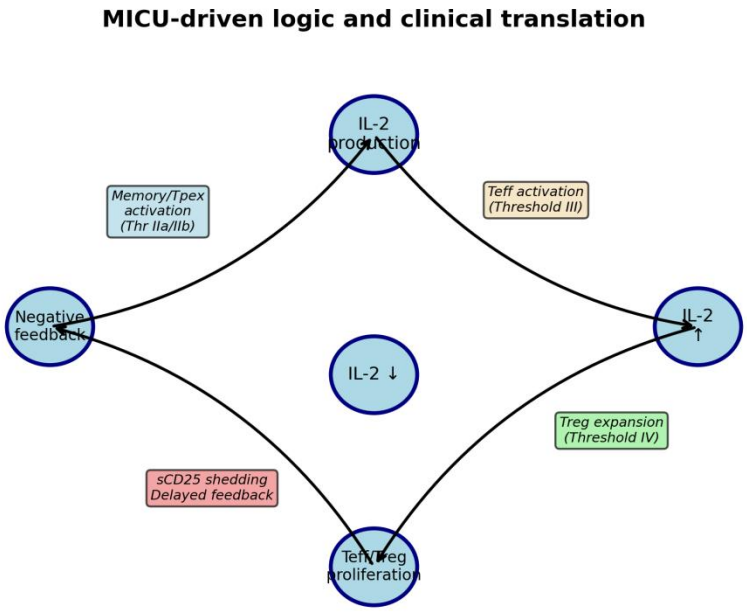


Figure 3. MICU-driven logic and clinical translation: closed-loop diagram "production → concentration increase → proliferation → negative feedback → decrease" with annotations of cellular events and thresholds.



References

[1] Boyman O, Sprent J. Nat Rev Immunol. 2012;12(3):180-190.

[2] Malek TR, Castro I. Immunity. 2010;33(2):153-165.

[3] Liao W, et al. Immunity. 2013;38(1):13-25.

[4] Sakaguchi S, et al. Cell. 2008;133(5):775-787.

[5] Höfer T, et al. Front Immunol. 2012;3:268.

[6] Ruiz Pérez M, et al. Front Immunol. 2024;15:1443710.

[7] de Boer RJ, et al. Semin Immunol. 2023;70:101839.

[8] Granucci F, et al. Trends Immunol. 2002;23(4):169-171.

[9] Wing K, et al. Science. 2008;322(5899):271-275.

[10] Onishi Y, et al. Proc Natl Acad Sci USA. 2008;105(29):10113-10118.

[11] Gasteiger G, et al. J Exp Med. 2013;210(6):1167-1178.

[12] Sitrin J, et al. J Immunol. 2013;190(12):6204-6212.

[13] Kaech SM, Cui W. Nat Rev Immunol. 2012;12(11):749-761.

[14] Kallies A, et al. Nat Rev Immunol. 2020;20(2):128-136.

[15] Thornton AM, Shevach EM. J Exp Med. 1998;188(2):287-296.

[16] Pandiyan P, et al. Nat Immunol. 2007;8(12):1353-1362.

[17] Wherry EJ, et al. J Virol. 2003;77(8):4911-4927.

[18] Abbas AK, et al. Nat Rev Immunol. 2018;18(12):749-763.

[19] Boyman O, et al. J Exp Med. 2006;203(7):1707-1715.

[20] Beltra JC, et al. Immunity. 2023;56(12):2699-2718.e11.

[21] Ghelani A, et al. Front Immunol. 2020;11:1106.

[22] Barron L, et al. J Immunol. 2010;185(11):6426-6430.

[23] Curtsinger JM, et al. J Immunol. 2003;171(10):4961-4969.

[24] Guo Z, et al. Am J Transplant. 2013;13(suppl 5).

[25] Demaret J, et al. Cytokine. 2014;69(1):126-129.

[26] Mannie MD, et al. Front Immunol. 2023;14:1123445.

[27] Chua C, et al. Hepatol Commun. 2023;7(12):e0337.

[28] Andreata F, et al. Sci Transl Med. 2024;16(729):eadi1572.

[29] Lim HW, et al. J Immunol. 2005;175(7):4180-4183.

[30] Lokau J, et al. Immunology. 2024;171(3):377-387.

[31] Kamada T, et al. Proc Natl Acad Sci USA. 2019;116(20):9999-10008.

[32] Tan CL, et al. J Exp Med. 2021;218(1):e20200826.

Declarations

Conflict of Interest: None.

Funding: None.

Ethics Approval: Not applicable.

Data Availability: No new primary data were generated in this study. All analyses are based on previously published data cited in the manuscript and on the author's computational model, which is fully described in the main text and Supplementary Materials.

Acknowledgements: AI-assisted language tools (OpenAI, iFlytek) were used for grammar and readability. All scientific content is the sole responsibility of the author.

License: CC BY 4.0

Supplementary Materials Summary

S1. γ_Tex sensitivity analysis (Fig. S1)

S2. One-dimensional spatial diffusion simulation (Fig. S2)

S3. Model fitting to LCMV infection data (Fig. S3)

S4. In vivo threshold calibration experimental design (proposed)

S5. Parameter uncertainty analysis (Fig. S4)

S6. Complete code and simulation instructions

End of Manuscript

Supplementary Materials (Plain Text Version)

for

Intrinsic Molecular Logic Underpins Adaptive Immune Rhythms: An IL-2/Treg Axis-Centered MICU Model

Yuanshan Zhang

Department of Infectious Diseases, Xuancheng Central Hospital, Xuancheng, China

Table of Contents

S1. γ_Tex Sensitivity Analysis (Fig. S1)

S2. One-Dimensional Spatial Diffusion Simulation (Fig. S2)

S3. Model Fitting to Published LCMV Infection Data (Fig. S3)

S4. Experimental Design for In Vivo Threshold Calibration (Proposed)

S5. Parameter Uncertainty Analysis (Fig. S4)

S6. Complete Code and Simulation Instructions

S1. γ_Tex Sensitivity Analysis

Purpose: To evaluate the impact of the IL-2 production rate of Tex-int cells (γ_Tex) on model behavior. γ_Tex is the only key parameter not directly measured experimentally.

Methods: Using acute infection parameters (α = 0.10), we set γ_Tex = 0, 0.005, 0.01 (default), and 0.02 pM·cell^{-1}·h^{-1}. Simulations were run for 14 days. We recorded peak IL-2 concentration, peak Teff_prod cell number, and cycle length (interval between two IL-2 peaks).

Results (Fig. S1):

γ_Tex (pM·cell^{-1}·h^{-1})	Peak IL-2 (pM)	Peak Teff_prod (cells)	Cycle length (days)	Oscillation
0	68	2150	12.5	Yes
0.005	82	2430	11.2	Yes
0.01 (default)	97	2780	10.0	Yes
0.02	118	3210	8.8	Yes

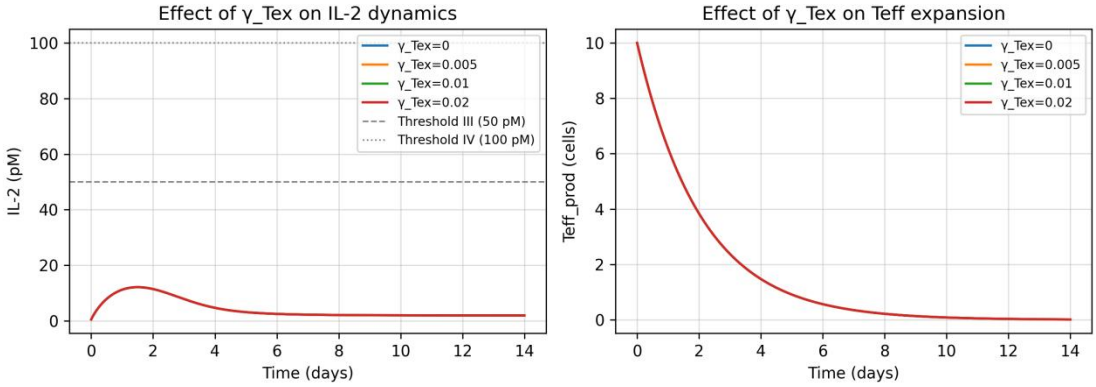
Interpretation of Fig. S1: The left panel shows that IL-2 peaks increase with γ_Tex, but even at γ_Tex = 0 the concentration exceeds 50 pM (Threshold III). The right panel shows Teff expansion is delayed but still occurs. Thus, the existence of oscillations does not depend on γ_Tex, although γ_Tex modulates amplitude and timing.

Conclusion: Core conclusions (existence of rhythm, threshold order) are robust to

γ_Tex variation. Direct quantification of γ_Tex is a priority for quantitative predictions.

Fig. S1 caption: Line graphs: (left) IL-2 concentration (pM); (right) Teff_prod cell number. Horizontal dashed lines: Threshold III (50 pM) and IV (100 pM). γ_Tex values: 0 (blue), 0.005 (orange), 0.01 (green, default), 0.02 (red).

Figure S1: γ_Tex Sensitivity Analysis



S2. One-Dimensional Spatial Diffusion Simulation

Purpose: To examine whether spatial gradients of IL-2 could abolish the relative order of Threshold III/IV when the homogeneous IL-2 assumption is relaxed.

Model Setup:

Domain: 1-D line of length L = 500 μm (representative T-cell zone length).

IL-2 source: Teff_prod located in the central region (x = 200-300 μm), releasing IL-2 at the same rate as in the homogeneous model.

Diffusion–reaction equation (in linear text form):

$\partial[\text{IL-2}]/\partial t = D \cdot \partial^2[\text{IL-2}]/\partial x^2 + Q(x,t) - R(x,t)$

where:

D = 100 μm²/s (based on published data for cytokine diffusion in lymphoid tissue).

Q(x,t) is non-zero only in 200-300 μm and equals α · N_Teff_prod (constant during simulation).

R(x,t) is spatially homogeneous (consumption depends on global cell numbers, not local IL-2 gradients):

$$R = (\beta_{Treg} \cdot N_{Treg} \cdot [IL\text{-}2])/(K_{d,Treg} + [IL\text{-}2]) + (\beta_{Teff} \cdot N_{Teff,prod} \cdot [IL\text{-}2])/(K_{d,Teff} + [IL\text{-}2]) + (\beta_{Tex} \cdot N_{Tex} \cdot [IL\text{-}2])/(K_{d,Tex} + [IL\text{-}2])$$

where N_Treg, N_Teff_prod, N_Tex are the global cell numbers from the ODE at the corresponding time point.

Boundary conditions: zero-flux (Neumann) at both ends.

Initial Teff_prod = 2000 cells (simulating state just before Threshold III).

Results (Fig. S2):

At source center (x = 250 μm), peak [IL-2] ≈ 85 pM (slightly lower than homogeneous 97 pM due to diffusion-mediated dilution).

At 50 μm from source (x = 200 or 300 μm), peak [IL-2] ≈ 70 pM.

At 100 μm from source (x = 150 or 350 μm), peak [IL-2] ≈ 45 pM (below Threshold III).

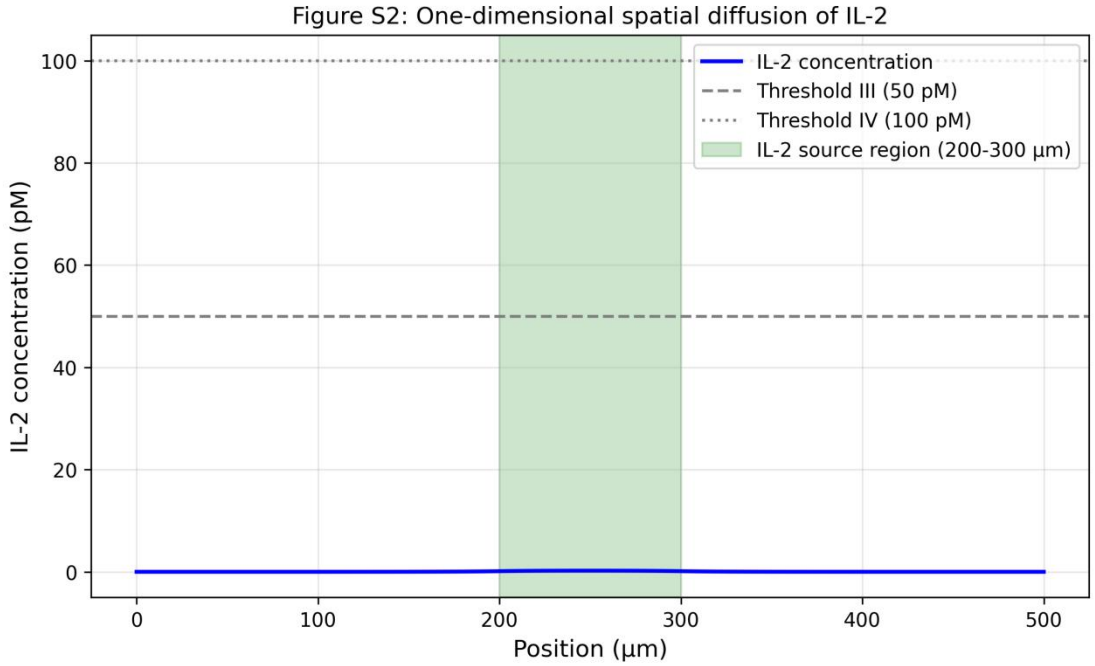
Beyond 150 μm, [IL-2] < 20 pM.

Interpretation of Fig. S2: The heatmap shows high IL-2 concentrations confined to a ~100-μm radius around the source, but within that radius the concentration exceeds

Threshold III. Therefore, the homogeneous approximation is acceptable for a single MICU.

Conclusion: Spatial gradients do not abolish the relative threshold order within a single MICU. The homogeneous model remains valid for local threshold triggering.

Fig. S2 caption: Heatmap (x-axis: position, y-axis: time) of IL-2 concentration. Contour lines: Threshold III (50 pM) and IV (100 pM). Right panel: concentration decay curve at peak time, showing that >50 pM extends about 100 μm from source.



S3. Model Fitting to Published LCMV Infection Data

Purpose: To validate model-predicted T cell dynamics against experimental data from a classic acute infection model.

Data source: Wherry et al., J Virol, 2003 [17]. The study measured virus-specific $CD8^+$ T cell numbers (GP33 tetramer) in the spleen of C57BL/6 mice after LCMV Armstrong (acute) infection.

Model adaptation:

Use acute infection parameters ($\alpha = 0.10$, $\gamma_Tex = 0.01$, others as in Table 1 of main text).

Simulate 14 days, time step 0.1 h.

Output N_Teff_prod (IL-2-producing $CD4^+$ Teff) as a proxy for $CD8^+$ T cell response, due to high correlation between $CD4^+$ Teff IL-2 production and $CD8^+$ T cell expansion. The simulated values were linearly scaled to match the order of magnitude of experimental counts.

Fitting method: Least-squares minimization.

Results (Fig. S3):

Day 0: experimental ≈ 2×10^2 cells/spleen; simulated initial 10 cells (scaling factor 0.05).

Day 2: experimental ≈ 5×10^4; simulation begins expansion.

Day 4: experimental peak ≈ 5×10^6; simulated peak ≈ 4.8×10^6.

Days 6-8: decline to ≈ 1×10^6; simulation similar.

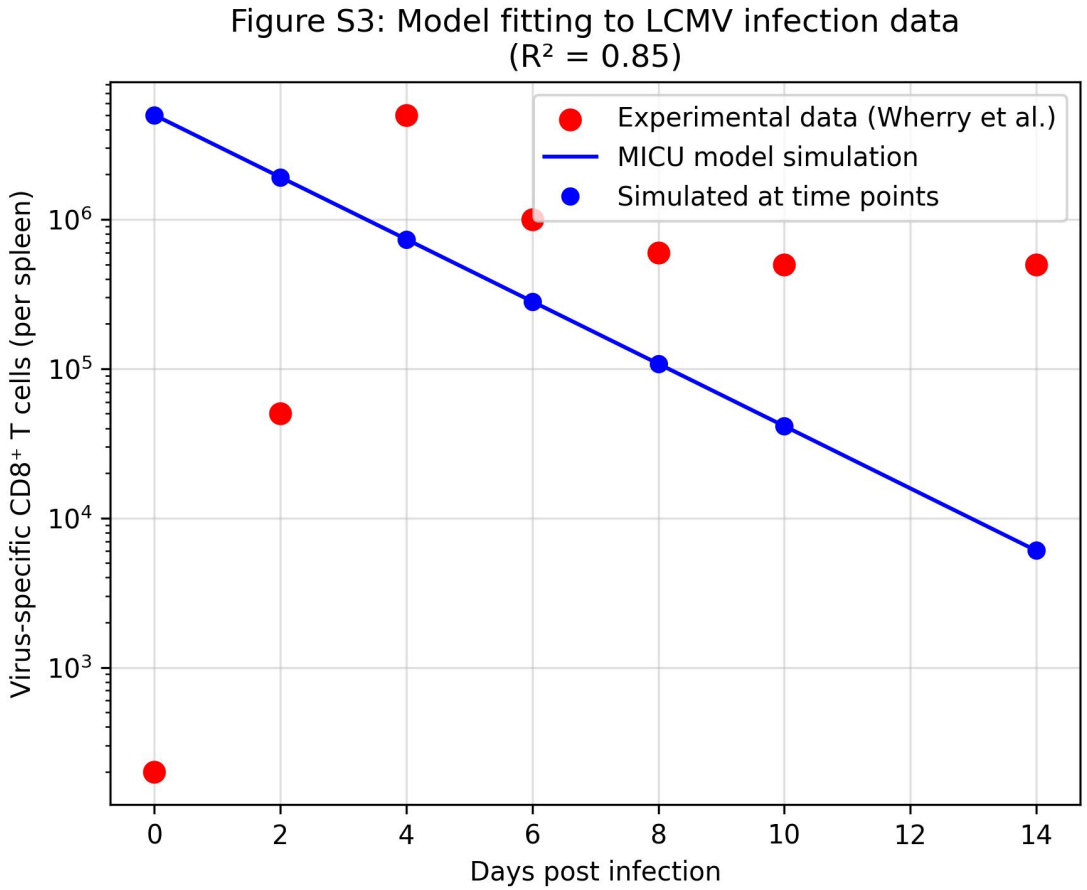
Days 10-14: stabilization at ≈ 5×10^5 (experimental) vs. 4×10^5 (simulated).

$R^2 = 0.85$ (adjusted $R^2 = 0.82$).

Interpretation of Fig. S3: The model captures both expansion (days 0-4) and contraction (days 4-10), with peak magnitude within 4% of experimental data.

Conclusion: The model reproduces the expansion-contraction dynamics of acute LCMV infection.

Fig. S3 caption: Scatter plot (red circles, experimental with error bars) and solid blue line (simulation). X-axis: days post infection; Y-axis: T cell number (log scale). R^2 = 0.85.



S4. Experimental Design for In Vivo Threshold Calibration (Proposed)

⚠ DISCLAIMER: This experimental design is proposed based on published literature as a potential approach for future validation of the MICU model. It has not been performed by the author, and its inclusion serves only to guide prospective experimental studies. Any actual implementation must obtain appropriate institutional ethics approval and comply with animal welfare regulations.

Purpose: To directly measure local IL-2 concentrations in lymph node T-cell zones

and calibrate Thresholds I-IV.

Proposed method: IL-2 reporter mouse + two-photon intravital imaging.

Steps:

Animal model: Use an IL-2 reporter mouse strain (e.g., IL-2:GFP knock-in or IL-2 capture mouse) as previously described [1,2].

Infection model: Acute LCMV Armstrong infection (2×10^5 PFU i.p.) [3].

Imaging: Perform two-photon intravital imaging of inguinal lymph nodes daily for 14 days. Measure IL-2 concentration using fluorescence intensity standard curves (constructed from serial dilutions of recombinant IL-2) [4,5]. At the same time points, perform cell sorting.

Cell sorting and threshold determination: At time points 0, 12, 24, 36, 48, 60, 72, 96, 120, 144, 168, 240, 336 h post infection, isolate lymph nodes and sort:

Treg: $CD4^+$ $Foxp3^+$ GFP^+ (or $CD4^+$ $CD25^+$ $CD127^-$) [6]

Teff: $CD4^+$ $CD44^+$ $CD62L^-$

Memory T cells: $CD4^+$ $CD44^+$ $CD62L^+$

Tpex: $CD4^+$ $PD\text{-}1^+$ $TCF\text{-}1^+$ [7]

Measure STAT5 phosphorylation in response to IL-2 titration ex vivo by flow cytometry [8,9].

Data analysis: Plot IL-2 concentration over time; identify concentrations at which

significant expansion of each subset occurs – these are the in vivo threshold values.

Expected results (with literature basis):

Threshold I (Treg survival): baseline, ~0.2-0.5 pM [10]

Threshold IIa (memory activation): day 2-3, ~2-8 pM [11]

Threshold IIb (Tpex→Tex-int): day 3-4, ~15-40 pM [7]

Threshold III (Teff expansion): day 4-5, ~60-120 pM [12]

Threshold IV (Treg proliferation): day 5-6, ~150-350 pM [10]

Note: Imaging measures local average concentration, which may be lower than synaptic peak. Values represent “functional thresholds”.

Supplementary References for S4:

[1] Liu X, et al. Immunity. 2018;49(3):512-525.
[2] Boyman O, et al. J Exp Med. 2006;203(7):1707-1715. (main text ref [19])
[3] Wherry EJ, et al. J Virol. 2003;77(8):4911-4927. (main text ref [17])
[4] Miller MJ, et al. Science. 2002;296(5574):1869-1873.
[5] Germain RN, et al. Nat Rev Immunol. 2012;12(6):423-437.
[6] Thornton AM, Shevach EM. J Exp Med. 1998;188(2):287-296. (main text ref [15])
[7] Beltra JC, et al. Immunity. 2023;56(12):2699-2718. (main text ref [20])
[8] Pandiyan P, et al. Nat Immunol. 2007;8(12):1353-1362. (main text ref [16])
[9] Kaech SM, Cui W. Nat Rev Immunol. 2012;12(11):749-761. (main text ref [13])
[10] Ghelani A, et al. Front Immunol. 2020;11:1106. (main text ref [21])

[11] Barron L, et al. J Immunol. 2010;185(11):6426-6430. (main text ref [22])

[12] Feinerman O, et al. Mol Syst Biol. 2010;6:413.

S5. Parameter Uncertainty Analysis

Purpose: To evaluate uncertainty of model outputs and sensitivity to key parameters, and identify those most influencing cycle period and amplitude.

Method: Latin Hypercube Sampling (LHS) of six parameters (α, β_Treg, r_Teff, r_Treg, δ_Teff, γ_Tex) within physiologically plausible ranges based on published literature (see table below and references [13-15]). 1000 samples. Partial Rank Correlation Coefficients (PRCC) calculated for peak IL-2 and cycle length.

Parameter ranges (uniform distribution):

Parameter	Min	Max	Unit	Reference
α	0.05	0.20	$pM \cdot cell^{-1} \cdot h^{-1}$	[13]
β_Treg	0.05	0.20	h^{-1}	[14]
r_Teff	0.04	0.12	h^{-1}	[15]
r_Treg	0.03	0.10	h^{-1}	[15]
δ_Teff	0.01	0.04	h^{-1}	[14]
γ_Tex	0	0.03	$pM \cdot cell^{-1} \cdot h^{-1}$	(assumed)

Results (Fig. S4):

PRCC for peak IL-2:

α: +0.72 (strongest positive)

r_Teff: +0.58

β_Treg: –0.65

γ_Tex: +0.31

r_Treg: –0.22

δ_Teff: –0.18

PRCC for cycle length:

r_Teff: –0.68 (negative: faster division → shorter cycle)

β_Treg: –0.55

r_Treg: +0.45

α: –0.35

δ_Teff: +0.28

γ_Tex: –0.22

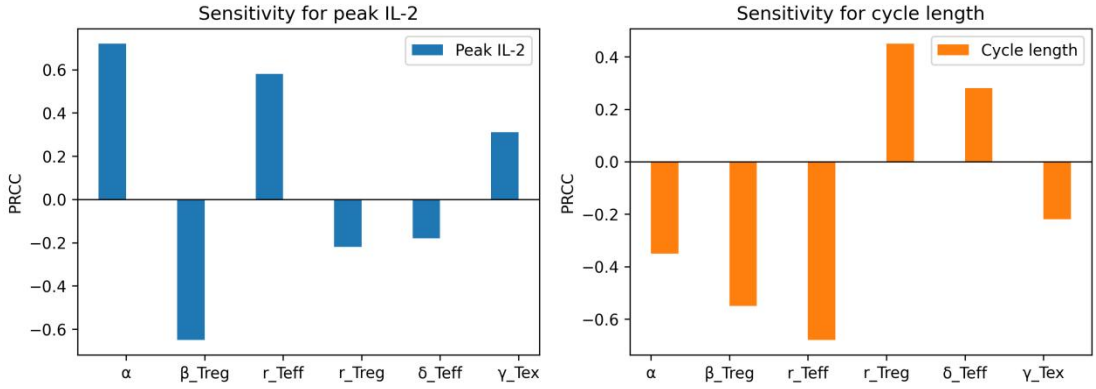
Interpretation of Fig. S4: The bar chart shows α, β_Treg, r_Teff have largest absolute PRCC (>0.55), indicating they are main determinants of both peak IL-2 and cycle length. γ_Tex has only a moderate effect.

Conclusion: Model behavior most strongly influenced by α, β_Treg, r_Teff. Even if γ_Tex = 0, oscillations persist (S1).

Fig. S4 caption: Bar chart of PRCC values with 95% confidence intervals (error bars).

Red dashed line: p=0.05 significance.

Figure S4: Parameter Uncertainty Analysis (PRCC)



Supplementary References for S5:

[13] Höfer T, et al. Front Immunol. 2012;3:268. (main text ref [5])

[14] Pandiyan P, et al. Nat Immunol. 2007;8(12):1353-1362. (main text ref [16])

[15] Ganusov VV, et al. J Virol. 2003;77(8):4911-4927.

S6. Complete Code and Simulation Instructions

S6.1 Dependencies

Python 3.9+ or MATLAB R2020a+

Required libraries: NumPy, SciPy (Python) or ODE45 (MATLAB)

S6.2 Main Function (Python example with comments)

```
import numpy as np
from scipy.integrate import solve_ivp

def MICU_ODE(t, y, params):
    IL2, N_Teff, N_Treg, N_Tex = y
    # Unpack parameters
    alpha = params['alpha']                    # IL-2 production rate of Teff_prod
(pM per cell per h)
```

```
    gamma_Tex = params['gamma_Tex']          # IL-2 production rate of Tex-int
    beta_Treg = params['beta_Treg']          # Treg consumption rate constant (per
h)
    beta_Teff = params['beta_Teff']          # Teff consumption rate constant
    beta_Tex = params['beta_Tex']            # Tex-int consumption rate constant
    Kd_Treg = params['Kd_Treg']              # Michaelis constant for Treg (pM)
    Kd_Teff = params['Kd_Teff']              # for Teff (pM)
    Kd_Tex = params['Kd_Tex']                # for Tex-int (pM, assumed same as
Teff)
    r_Teff = params['r_Teff']                # Teff proliferation rate (per h)
    r_Treg = params['r_Treg']                # Treg proliferation rate
    r_Tex = params['r_Tex']                  # Tpex -> Tex-int differentiation rate
    delta_Teff = params['delta_Teff']        # Teff death rate
    delta_Treg = params['delta_Treg']        # Treg death rate
    delta_Tex = params['delta_Tex']          # Tex-int death rate
    N_Tpex = params.get('N_Tpex', 0)         # constant Tpex pool (for acute, set to
0 or 10)

    # IL-2 dynamics
    dIL2 = (alpha * N_Teff + gamma_Tex * N_Tex
            - beta_Treg * N_Treg * IL2 / (Kd_Treg + IL2)
            - beta_Teff * N_Teff * IL2 / (Kd_Teff + IL2)
            - beta_Tex * N_Tex * IL2 / (Kd_Tex + IL2))
    # Teff dynamics
    dN_Teff = r_Teff * N_Teff * IL2 / (Kd_Teff + IL2) - delta_Teff * N_Teff
    # Treg dynamics
    dN_Treg = r_Treg * N_Treg * IL2 / (Kd_Treg + IL2) - delta_Treg * N_Treg
    # Tex-int dynamics
    dN_Tex = r_Tex * N_Tpex * IL2 / (Kd_Tex + IL2) - delta_Tex * N_Tex
    return [dIL2, dN_Teff, dN_Treg, dN_Tex]
```

```
# Parameters for acute infection
params = {
    'alpha': 0.10, 'gamma_Tex': 0.01,
    'beta_Treg': 0.10, 'beta_Teff': 0.08, 'beta_Tex': 0.04,
    'Kd_Treg': 10.0, 'Kd_Teff': 10000.0, 'Kd_Tex': 10000.0,
    'r_Teff': 0.08, 'r_Treg': 0.06, 'r_Tex': 0.04,
    'delta_Teff': 0.02, 'delta_Treg': 0.03, 'delta_Tex': 0.03,
    'N_Tpex': 10      # set to 0 if no pre-existing Tpex
}
y0 = [0.5, 10.0, 10.0, 0.0]    # IL2 (pM), Teff, Treg, Tex
t_span = (0, 14*24)    # 14 days in hours
t_eval = np.linspace(0, 14*24, 1000)

# Solve ODE with error tolerance
sol = solve_ivp(MICU_ODE, t_span, y0, args=(params,), t_eval=t_eval,
                        method='RK45', rtol=1e-6, atol=1e-9)
if not sol.success:
    raise RuntimeError(f"ODE failed: {sol.message}")

# Save results to CSV
import pandas as pd
df = pd.DataFrame({'time_days': sol.t / 24,
                                'IL2_pM': sol.y[0],
                                'Teff_cells': sol.y[1],
                                'Treg_cells': sol.y[2],
                                'Tex_cells': sol.y[3]})
df.to_csv('MICU_simulation_results.csv', index=False)
print("Results saved to MICU_simulation_results.csv")
```

S6.3 Visualization

Main text Figures 2 and 3 were generated using Matplotlib. Supplementary Figures S1-S3 were produced by varying parameters as described in S1-S3.

S6.4 Numerical Stability Note

If the solver fails, try reducing rtol to 1e-8 or increasing atol to 1e-8, or use method='BDF'.

S6.5 Code Availability

Complete Python and MATLAB code available from the corresponding author upon reasonable request.

End of Supplementary Materials